OPEN ACCESS Freely available online

PLoS one

Protective Role of Hydrogen Sulfide against Noise-Induced Cochlear Damage: A Chronic Intracochlear Infusion Model

Xu Li[1☯], Xiao-Bo Mao[1☯], Ren-Yi Hei[1], Zhi-Bin Zhang[2], Li-Ting Wen[1], Peng-Zhi Zhang[1], Jian-Hua Qiu[1]*, Li Qiao[1]*

1 Department of Otolaryngology-Head and Neck Surgery, Xijing Hospital, Fourth Military Medical University, Xi'an, China, **2** Perimed China Ltd, Beijing, China

Abstract

Background: A reduction in cochlear blood flow plays an essential role in noise-induced hearing loss (NIHL). The timely regulation of cochlear perfusion determines the progression and prognosis of NIHL. Hydrogen sulfide (H_2S) has attracted increasing interest as a vasodilator in cardiovascular systems. This study identified the role of H_2S in cochlear blood flow regulation and noise protection.

Methodology/Principal Findings: The gene and protein expression of the H_2S synthetase cystathionine-γ-lyase (CSE) in the rat cochlea was examined using immunofluorescence and real-time PCR. Cochlear CSE mRNA levels varied according to the duration of noise exposure. A chronic intracochlear infusion model was built and artificial perilymph (AP), NaHS or DL-propargylglycine (PPG) were locally administered. Local sodium hydrosulfide (NaHS) significantly increased cochlear perfusion post-noise exposure. Cochlear morphological damage and hearing loss were alleviated in the NaHS group as measured by conventional auditory brainstem response (ABR), cochlear scanning electron microscope (SEM) and outer hair cell (OHC) count. The highest percentage of OHC loss occurred in the PPG group.

Conclusions/Significance: Our results suggest that H_2S plays an important role in the regulation of cochlear blood flow and the protection against noise. Further studies may identify a new preventive and therapeutic perspective on NIHL and other blood supply-related inner ear diseases.

Citation: Li X, Mao X-B, Hei R-Y, Zhang Z-B, Wen L-T, et al. (2011) Protective Role of Hydrogen Sulfide against Noise-Induced Cochlear Damage: A Chronic Intracochlear Infusion Model. PLoS ONE 6(10): e26728. doi:10.1371/journal.pone.0026728

Editor: Li I. Zhang, University of Southern California, United States of America

Received April 29, 2011; **Accepted** October 2, 2011; **Published** October 26, 2011

Funding: This study was supported by the grants from the National Natural Science Foundation of China (No. 30973299, 81070791, 30872857, and 30930098). Jian-Hua Qiu and Li Qiao were the recipients of the grants. The funders had no role in study design, data collection and analysis, decision to publish, or preparation of the manuscript.

Competing Interests: Perimed Ltd. offered PSI laser speckle contrast blood perfusion imager and consultancy services in this study. Zhi-Bin Zhang is an employee of Perimed China Ltd. This does not alter the authors' adherence to all the PLoS ONE policies on sharing data and materials.

* E-mail: qiujh@fmmu.edu.cn (J-HQ); qiaoli@fmmu.edu.cn (LQ)

☯ These authors contributed equally to this work.

Introduction

Noise-induced hearing loss (NIHL) is a sensorineural hearing loss that results from noise-induced cochlear hair cell damage. An increasing number of individuals suffer from NIHL, which creates a great economic burden and a poor quality of life. Therefore, an investigation of the prevention and potential therapies of NIHL is warranted.

Temporary or permanent sensorineural hearing loss that is induced by exposure to noise depends on multiple factors, including noise parameters, living habits and genetic susceptibility [1,2]. Although the exact pathological mechanism of NIHL is not known, direct mechanical trauma, metabolic stress and disorders of cochlear blood flow have been suggested [3–5]. Interestingly, each of these theories involves a disability of cochlear microvascular regulation, which may play an important role in NIHL. Vascular regulation includes vasoconstriction and vasodilation. Endothelin, α-adrenergic receptors, peptide-containing nerve fibers, and sphingosine-1-phosphate receptors participate in the constriction of spiral modiolar artery (SMA) [6–12], and nitric oxide (NO) and calcitonin gene-related protein (CGRP) regulate the relaxation of SMA [13,14]. However, these factors do not exert a vasodilator effect on the SMA that is timely, rapid and strong enough to provide cochlear protection against noise.

Hydrogen sulfide (H_2S) is a poisonous and occasionally lethal gas that is physiologically synthesized in blood vessels by cystathionine-γ-lyase (CSE) from L-cysteine. H_2S activates ATP-sensitive potassium channel (K_{ATP}) and transient receptor potential (TRP) channels to exert vasodilatory effects [15], which may be initiated by hypoxia [16]. CSE knockout mice display hypertension and diminished endothelium-dependent vasodilation [17]. The administration of DL-propargylglycine (PPG), which is an inhibitor of CSE, recovers arterial pressure and heart rate in rats [18]. These results suggest that H_2S is a physiological vasodilator.

However, whether H_2S assumes the same responsibility in the cochlea remains to be elucidated. This study explored the

regulatory effect of H_2S on cochlear blood flow and identified the potential protective role of H_2S against NIHL. These results provide a new preventive and therapeutic perspective for blood supply-related inner ear diseases.

Results

CSE protein expression in cochlea

Immunofluorescence was used to examine the protein expression of CSE in cochlea. CSE protein was identified in the cochlear stria vascularis and the SMA wall (Fig. 1A). No immunofluorescence was observed in controls. The distribution of CSE protein corresponded with previous reports of CSE expression in the cardiovascular system [19].

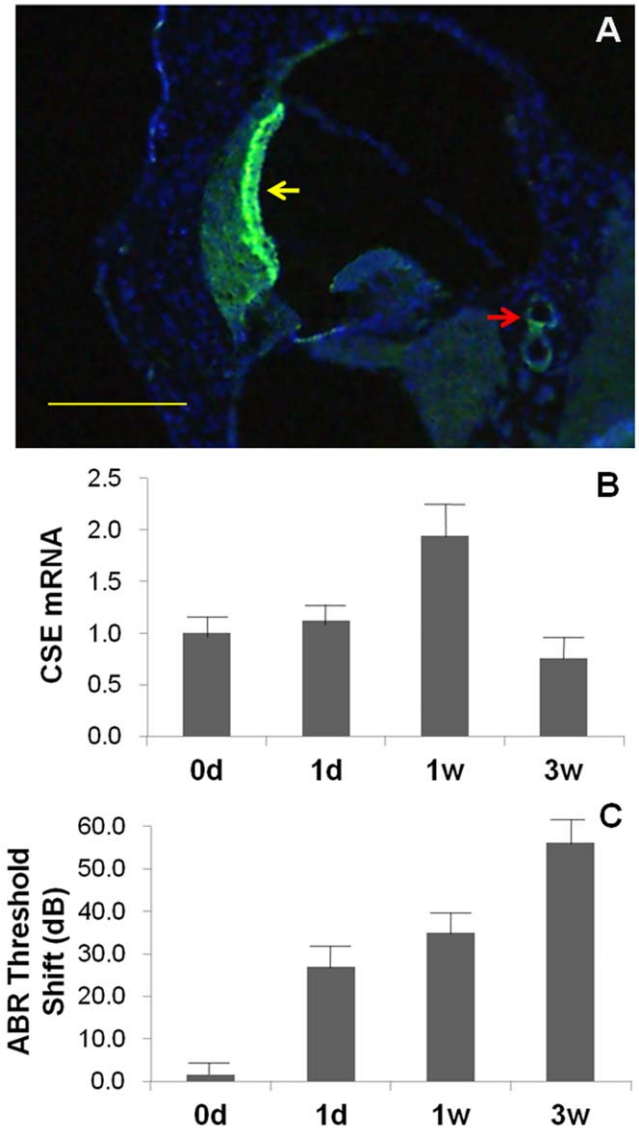

Figure 1. CSE expression in cochlea. A: Immunofluorescent photograph of CSE in the cochlea (bar = 200 μm). CSE protein was positively expressed in the stria vascularis (yellow arrow) and the wall of the spiral modiolar artery (red arrow). B and C are mean CSE mRNA expression in rat cochlea and ABR threshold shifts. The relative expressions after noise exposure for 0 d, 1 d, 1 w and 3 w were 1.00±0.17, 1.12±0.17, 1.95±0.31 and 0.76±0.19, respectively. ABR threshold shifts were 1.56±3.26, 26.88±5.79, 35.00±5.18 and 56.25±5.67 dB SPL, respectively. They both increased with increased exposure time initially. In the 3-week exposure group, the expression of CSE mRNA decreased inversely.
doi:10.1371/journal.pone.0026728.g001

Cochlear CSE mRNA expression after different durations of noise exposure

To show that H_2S may play a role in NIHL, cochlear CSE mRNA expression and auditory brainstem response (ABR) threshold shifts were analyzed after different durations of noise exposure. Cochlear CSE mRNA was assessed using real-time quantitative PCR, and the results are shown in Fig. 1B. CSE transcripts were detected in all samples. The relative expressions after noise exposure for 0 d, 1 d, 1 w and 3 w were 1.00±0.17, 1.12±0.17, 1.95±0.31 and 0.76±0.19, respectively. ABR threshold shifts were 1.56±3.26, 26.88±5.79, 35.00±5.18 and 56.25±5.67 dB SPL, respectively (Fig. 1C). CSE mRNA expression and ABR threshold shifts increased with the increased in exposure time when the noise stimulation lasted no more than 1 week. However, CSE mRNA expression decreased inversely in the 3-week exposure group. We ascribed this decrease to cochlear decompensation that resulted from noise overstimulation.

H_2S donor increased cochlear blood flow

To reveal the effect of noise, the cochlear blood flow was detected in 7 cochleae before and after noise exposure. Post-exposure data were also recorded after previous sodium hydrosulfide (NaHS) or artificial perilymph (AP) administration to identify the effect of H_2S. Blood perfusion image (Fig. 2A), color photograph (Fig. 2B) and blood flow (Fig. 2C) were presented respectively. An evident blood flow reduction was observed immediately after noise exposure compared to the pre-exposure blood flow. A progressive increase and gradual recovery was observed in the following 15–20 min. ANOVA indicated a significant difference in cochlear blood flow between control, AP, and NaHS administration ($F = 26.79$, $p<0.001$). Cochlear post-exposure blood flow after NaHS administration increased significantly compared to the administration of AP (SNK test, $p<0.05$) (Fig. 2D). The same result was observed using laser Doppler flowmetry (PeriFlux System 5000 and Probe 401; Perimed, Stockholm, Sweden).

Morphological and functional protection of H_2S against NIHL

A chronic intracochlear infusion model was built and AP, NaHS or DL-propargylglycine (PPG) was locally administered. To identify the morphological and functional protection of H_2S against NIHL, ABR measurement, scanning electron microscope (SEM) and outer hair cell (OHC) count were carried out.

Two rats died of post-surgical infection, and one rat died of hemorrhage. The ABR threshold shifts immediately after surgery in the control[1], NaHS[2] and PPG[3] groups were 7.78±1.88, 6.50±1.30 and 5.00±1.34 dB SPL, respectively. No significant differences between groups were observed (Equivalence test, $0.002<P_{1,\ 2}<0.005$, $P_{2,\ 3}<0.001$, $0.002<P_{1,\ 3}<0.005$).

SEM and cochlear surface preparation revealed missing hair cells primarily in OHCs but seldom in inner hair cells (IHCs) (Figs. 3A–C, G–I). The missing OHCs were localized primarily in the superior segment of the basal turn. In contrast to the evident stereocilia bundle defects in the control (Figs. 3D and G) or PPG (Figs. 3F and I) groups, the stereocilia bundles appeared reasonably normal in the NaHS group (Figs. 3E and H). The percent OHC loss in each row is listed in Fig. 3J. OHC loss was localized in the third row and the posterior second row, which

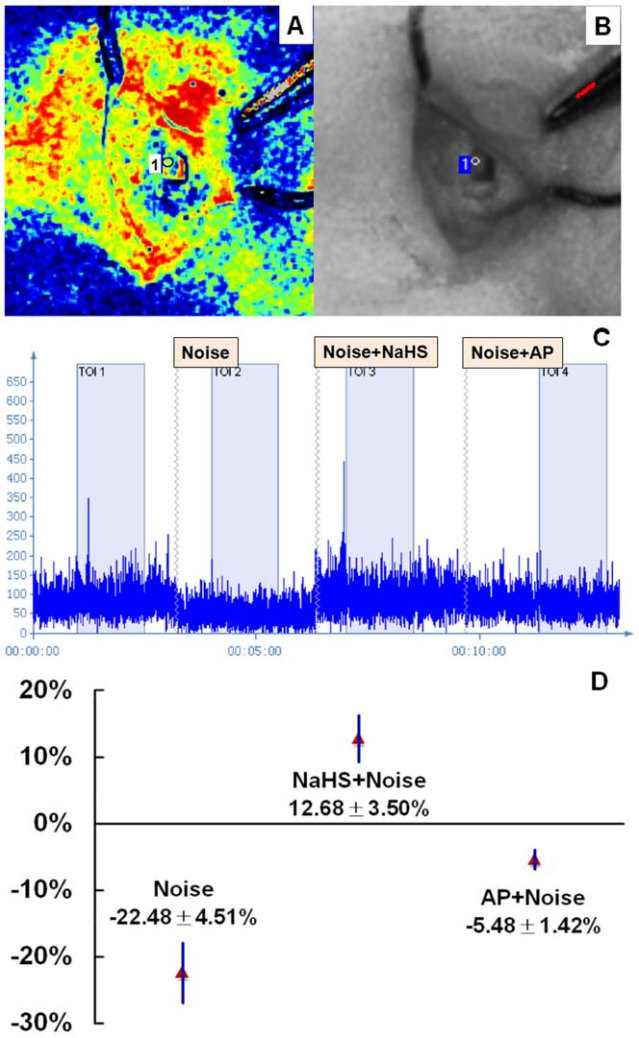

Figure 2. Detection of cochlear blood perfusion. The cochlear blood flow was detected before and after noise exposure. Post-exposure data were also recorded after previous NaHS or AP administration to identify the effect of H_2S. A and B are a recorded blood perfusion image and color photograph, respectively. C represents cochlear blood flow in graphical form. X axis is time and Y axis is blood flow data. A blood flow reduction was observed immediately after noise exposure compared to the pre-exposure blood flow. D shows changes in post-exposure cochlear blood flow after different interventions. Cochlear post-exposure blood flow after NaHS administration increased significantly compared to that after AP administration ($n = 7$, $P<0.05$).
doi:10.1371/journal.pone.0026728.g002

demonstrated a different susceptibility of the OHCs in each row to noise. Statistical analyses revealed that the percent of OHC loss in the first row increased in the PPG group and decreased significantly in the NaHS group (ANOVA, $F = 11.83$, $p<0.01$; SNK test, $p<0.05$). The disarrangement of OHC stereociliary bundles was least obvious in the NaHS group compared to the other groups. These results suggested that exogenous H_2S administration protected the cochlea against noise damage.

The ABR threshold shifts of post-surgical rats were recorded at different times after noise exposure (Fig. 3K). The auditory system recovered gradually. ANOVA indicated a significant difference in the ABR shift on the 14th day between the three groups ($F = 4.71$, $p<0.05$). There was no statistically significant difference between the control group (56.11±2.32 dB SPL) and the PPG group (56.88±2.82 dB SPL) (SNK, $P>0.05$). However, the ABR threshold shift demonstrated a significant decrease in the NaHS group (47.00±2.60 dB SPL) compared to the other groups (SNK, $P<0.05$). These results suggested a functionally protective effect of H_2S against NIHL.

Discussion

This study explored the potential action of H_2S in the cochlea. The results demonstrated that the CSE protein was expressed abundantly in rat cochlea. CSE mRNA expression correlated with the duration of noise stimulation, which suggested its probable association with acoustic trauma. Exogenous H_2S increased cochlear blood flow rapidly, which may relieve noise-induced blood flow decrease. The intracochlear administration of an H_2S donor ameliorated noise-induced cochlear morphological damage and hearing impairment. Therefore, H_2S may morphologically and functionally protect the cochlea against noise-induced damage. We conclude that the protection may result from its effect of cochlear microcirculation improvement.

H_2S is a well-known environmental hazard and toxin. However, its essential physiological role as an endogenous gaseous transmitter has garnered much attention. H_2S induces either relaxation or contraction depending on different concentrations and vessel type [20–23]. H_2S regulates angiogenesis under physiological and ischemic conditions [24], and it may play an important role in atherosclerosis [25]. H_2S demonstrates cytoprotective effect in various organ systems in ischemia/reperfusion injury [26]. Furthermore, H_2S may exert a different action in various inflammatory states [27–29].

CSE activity determines H_2S production in cardiovascular system. The timely, rapid and strong vasodilator effect of H_2S likely satisfies the needs of cochlear blood flow autoregulation. The CSE inhibitor, PPG, regulates the endogenous production of H_2S [30,31]. In this study, cochlear protection was mainly induced by exogenous H_2S, but the action of PPG was not obvious. We hypothesize that the greater loss of OHCs resulted from the direct action of PPG.

A laser speckle contrast blood perfusion imager was used to detect cochlear blood flow in this study. In contrast to laser Doppler flowmetry, the laser speckle contrast blood perfusion imager visualizes tissue blood perfusion in real-time and combines dynamic responses with spatial resolution.

Our results revealed the expression of CSE in the cochlea and the role of H_2S in the regulation of cochlear blood flow. Further studies may provide a new preventive and therapeutic perspective on NIHL and other blood supply-related inner ear diseases.

Materials and Methods

Animals and Ethics Statement

SD rats weighing 250–350 g were used in this study. All rats were provided by the animal center of the Fourth Military Medical University and had free access to water and food. All procedures concerning animals in this study were approved by the Institutional Animal Care and Use Committee of the Fourth Military Medical University (Permit number, SYXK 2008-005) in compliance with the Guide for the Care and Use of Laboratory Animals.

Immunological studies

Rats were anesthetized with a 50 mg/kg intraperitoneal injection of sodium pentobarbital (catalog number P11011, Merck, Germany). Perfusions through the heart were performed with freshly prepared 4% phosphate-buffered paraformaldehyde

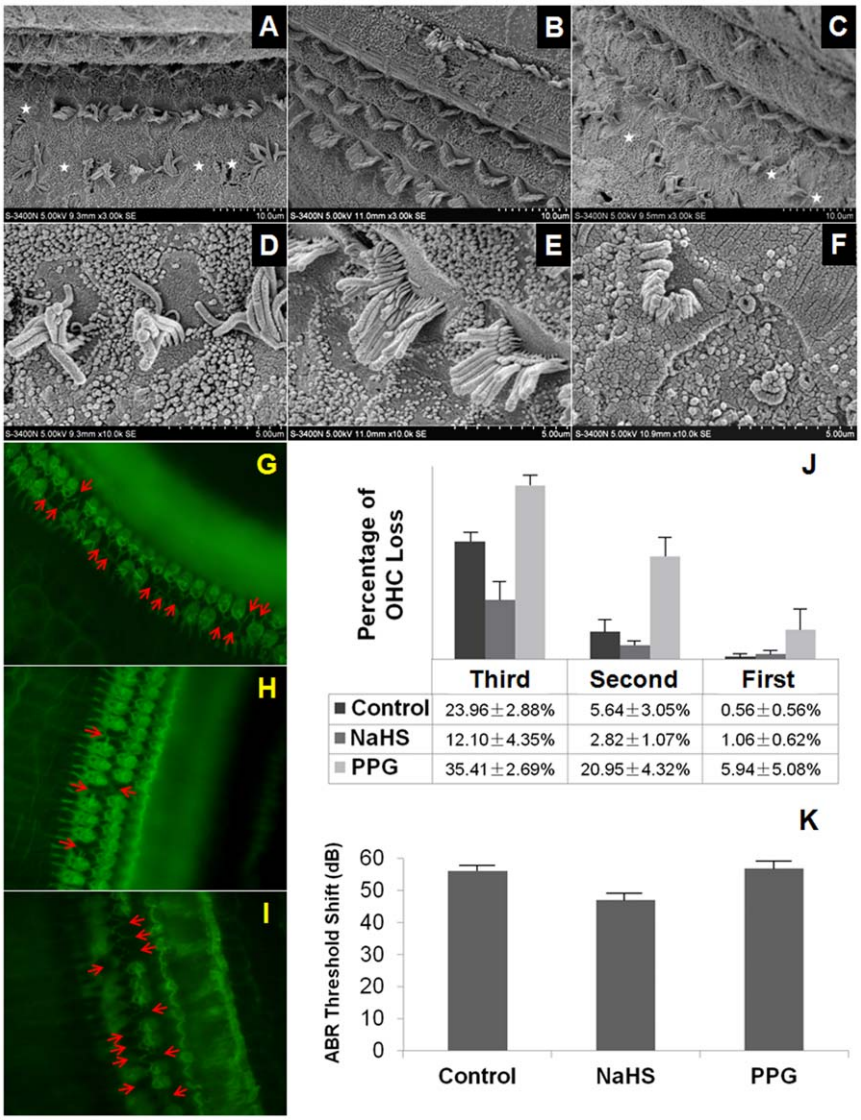

Figure 3. Morphological and functional protective effects of H_2S against NIHL. A–F: Scanning electron micrographs of the basilar membrane. Evident stereocilia bundle defects (white stars) were observed in control (D, E) and PPG (H, I) groups. The stereocilia bundles in the NaHS group appeared relatively normal (F, G). G–I: Cochlear sensory epithelia surface preparation in control (A), NaHS (B) and PPG (C) groups. OHC loss and evident stereocilia bundle defects are indicated (red arrows). J: Percent OHC loss in each row. The loss was localized primarily in the third row and the posterior second row. OHC loss in the NaHS group is less than control. The PPG exhibited the highest loss percentage. K: Mean post-surgical ABR threshold shifts at different time points after noise exposure. The ABR threshold shift demonstrated a significant decrease on the 14th day in the NaHS group (47.00±2.60 dB SPL) compared to the control group (56.11±2.32 dB SPL) and the PPG group (56.88±2.82 dB SPL) ($P<0.05$).
doi:10.1371/journal.pone.0026728.g003

(pH 7.4). The temporal bones were removed immediately and were post-fixed in the same solution overnight. After decalcification in 10% ethylene diamine tetraacetic acid (EDTA) for 7 d and dehydration in 30% sucrose for 24 h, immunofluorescence was performed on cochlear frozen sections (8 μm thickness). The sections were blocked with 0.3% peroxide in methanol and 10% normal goat serum successively. The sections were incubated overnight at 4°C with a mouse monoclonal anti-CSE antibody (catalog number H00001491-M01, Abnova, Taiwan, China). A fluorescein isothiocyanate (FITC)-conjugated goat anti-mouse IgG (Sigma Chemical Co., St. Louis, MO, USA) was used as a secondary antibody. A Hoechst (Sigma Chemical Co., St. Louis, MO, USA) was used to stain the nucleus. After several rinses in PBS, the sections were photographed using an Olympus BX51 compound microscope.

Noise exposure

Rats were separately placed into wire mesh cages in a ventilated chamber with free access to food and water during noise exposure. A RadioShack Super-tweeter located above the cages generated a noise (4 kHz octave band, 120 dB SPL) for 6 h. The noise was amplified using a power amplifier (Yamaha AX-500U) and delivered to a loudspeaker. The homogeneity of the sound field was confirmed using a sound-level meter (Bruel and Kjaer Type 2606) that was placed at various locations within the chamber.

ABR measurements

After an intraperitoneal injection of sodium pentobarbital (40 mg/kg), the reference, ground and active needle electrodes

were inserted beneath the skin of the post-measured auricle, the sacrococcygeal region and the calvaria, respectively. The responses to 1024 click presentations were amplified, filtered, and synchronously averaged. Each stimulus was presented initially at 100 dB SPL. The stimulus intensity was decreased systematically in 5-dB steps until a visually discernible ABR waveform disappeared. 'Threshold' was defined as the lowest level of the stimulus that produced a visually detectable response.

RNA isolation and real-time quantitative PCR

Total RNA was isolated from the stria vascularis and basilar membrane using TRIZOL reagent (Takara Shuzo, Shiga, Japan). Reverse transcription was performed using a PrimeScript RT Master Mix (Takara Shuzo, Shiga, Japan) according to the manufacturer's instructions. Total RNA (1 μg) was reverse transcribed into cDNA in each sample. Controls that contained no reverse transcriptase were used to safeguard for genomic DNA contamination. Real-time PCR was performed in an iCycler iQ Real-time PCR Detection (Bio-Rad, Hercules, CA) associated with the iCycler optical system software (version 3.1) using SYBR Premix Ex Taq II according to the protocol. Briefly, all PCRs were performed in a volume of 25 μl. The cycling was conducted at 95°C for 90 s followed by 38 cycles of 95°C for 10 s and at 60°C for 20 s. The primers of CSE were as follows: sense 5′-AGCGATCACACCACA-GACCAAG-3′ and antisense 5′-ATCAGCACCCAGAGCCAAAGG-3′. These primers produced a product of 178 bp. The primers for rat β-actin were sense 5′-CGTTGACATCCGTAAAGAC-3′and antisense 5′-TAGGAGCCAGGGCAGTA-3′. Specificity of the amplification was determined using a melting curve analysis. Data are expressed as a ratio of the quantity of CSE mRNA to the quantity of β-actin mRNA using the arithmetic formula $2^{-\Delta\Delta CT}$.

Detection of cochlear blood flow

After deep anesthesia and post-auricular skin preparation, an incision was performed to expose the temporal bone. The bulla was opened to reveal the round window and the basal turn of the cochlea. The cochlear mucoperiosteum was uncovered under a microscope. Cochlear blood flow was recorded before and after noise exposure (120 dB SPL, 4 kHz for 10 min) using a laser speckle contrast blood perfusion imager (PeriCam PSI; Perimed, Stockholm, Sweden). Signal amplitudes that backscattered from the cochlea were calculated using the manufacturer's software (PimSoft 1.2.2.5676; Perimed, Stockholm, Sweden). A piece of gel foam (3 mm×3 mm) that was immersed in 0.3 ml AP or NaHS (1 mmol/L) was placed on the round window. Blood flow was detected again after the same noise stimulation was applied. Twenty-five min between neighboring noise exposures were reserved for the recovery of cochlear blood flow.

Surgery and experimental group

Thirty rats were divided randomly into 3 groups (control, NaHS and PPG group). The chronic intracochlear infusion models were designed according to the method described by Prieskorn et al. [32]. Briefly, the right post-auricular region was shaved and cleaned for surgical manipulation after deep anesthesia. Lidocaine hydrochloride (1%) was injected subcutaneously to provide local anesthesia. A post-auricular incision was performed, and the muscles were separated to expose the temporal bone. The bulla was perforated using a 1 mm diamond paste burr for visualization of the round window and the cochlear basal turn. A small fenestra was created using a sharpened probe on the basal turn of the scala tympani approximately 1.0 mm below the round window. The tip of a mouse jugular catheter (Order No.: 0007700, Alza Corp., CA, USA) was inserted into the scala tympani and connected to a mini-osmotic pump #2002 (Alza Corp., CA, USA), which was embedded hypodermically. The pumps and catheters were filled with 200 μl AP, NaHS (1 mol/L) or PPG (1 mol/L) 12 h before implantation and primed according to the manufacturer's recommendations. Sterile working conditions were maintained throughout the entire procedure. Animals were exposed to noise (120 dB SPL, 4 kHz, 6 h) the following day. The ABR thresholds were recorded pre-surgery and post-surgery on the 1st, 3rd, 5th, and 14th d after noise exposure. OHC counts and cochlear SEM were performed after the last ABR measurement.

Cochlear sensory epithelia surface preparation and OHC count

The animals were perfused transcardially with freshly prepared 4% phosphate-buffered paraformaldehyde (pH 7.4) under deep anesthesia. The right cochleae were removed immediately. Cochleae were perfused locally through the open round windows and cochlear apexes to ensure efficient fixative perfusion and post-fixed in the same stationary liquid overnight. After removal of the bony capsule, the spiral ligament, stria vascularis and Reissner's membrane were separated under a dissecting microscope. Each turn of the Corti organ was detached from the bony modiolus. The sensory epithelium was trimmed, and surface preparations were stained for actin using fluoresceinyl-aminomethyldithiolano-phalloidin (catalog number Alx-350-268-MC01, Enzo Life Sciences, Farmingdale, NY, USA). The sensory epithelia surface structures were carefully examined for missing cells or stereocilia under a fluorescence microscope (Olympus, Tokyo, Japan) at a magnification of 400×. The missing hair cells and stereocilia were quantified and photographed along the entire basilar membrane. The percent missing OHCs in each row were calculated and compared between the three groups.

SEM study

Deeply anesthetized animals were decapitated on the 15th day after noise exposure. The right cochleae were removed immediately and gently perfused with 2.5% phosphate-buffered glutaraldehyde (catalog number A17876, Alfa-Aesar, USA) (pH 7.4) through the open round window and the cochlear apex. The cochleae remained in the same solution overnight. The bony capsule was removed after washing with 0.1 M phosphate-buffered saline (PBS). The spiral ligament and stria vascularis were removed under a dissecting microscope. The Reissner's membrane was separated. The dissected specimens were rinsed with 0.1 M PBS, post-fixed in 1% osmium tetroxide for 2 h and placed in 2% tannic acid twice for 30 min. The cochleae were dehydrated in a series of graded ethanol solutions and dried in a critical point drier (hcp-2, Hitachi). The specimens were fixed on a metal stage, gold-coated in a sputter coater (E102 Ion Sputter, Hitachi) and observed under a SEM (Hitachi S-800).

Statistical analyses

Data are presented as the mean ± SE. The equivalence test assessed the interclass differences of surgical impact on the auditory system. ANOVA followed by the SNK test identified the differences between means. A value of $P<0.05$ was considered statistically significant. The analyses were performed using a commercial statistical software package (SPSS 13.0; SPSS Inc., Chicago, Ill.).

Acknowledgments

We thank Prof. YX Bai (Statistics Department of Fourth Military Medical University) for his constructive statistical advice.

Author Contributions

Conceived and designed the experiments: JHQ LQ. Performed the experiments: XL XBM RYH ZBZ LTW PZZ. Analyzed the data: XL LQ XBM. Wrote the paper: XL.

References

1. Fransen E, Topsakal V, Hendrickx JJ, Van Laer L, Huyghe JR, et al. (2008) Occupational noise, smoking, and a high body mass index are risk factors for age-related hearing impairment and moderate alcohol consumption is protective: a European population-based multicenter study. J Assoc Res Otolaryngol 9: 264–276.
2. Gratton MA, Eleftheriadou A, Garcia J, Verduzco E, Martin GK, et al. (2010) Noise-induced changes in gene expression in the cochleae of mice differing in their susceptibility to noise damage. Hear Res. In press.
3. Ohinata Y, Yamasoba T, Schacht J, Miller JM (2000) Glutathione limits noise-induced hearing loss. Hear Res 146: 28–34.
4. Le Prell CG, Yamashita D, Minami SB, Yamasoba T, Miller JM (2007) Mechanisms of noise-induced hearing loss indicate multiple methods of prevention. Hear Res 226: 22–43.
5. Nakashima T, Naganawa S, Sone M, Tominaga M, Hayashi H, et al. (2003) Disorders of cochlear blood flow. Brain Res Brain Res Rev 43: 17–28.
6. Scherer EQ, Arnold W, Wangemann P (2005) Pharmacological reversal of endothelin-1 mediated constriction of the spiral modiolar artery: a potential new treatment for sudden sensorineural hearing loss. BMC Ear Nose Throat Disord 5: 10.
7. Wangemann P, Wonneberger K (2005) Neurogenic regulation of cochlear blood flow occurs along the basilar artery, the anterior inferior cerebellar artery and at branch points of the spiral modiolar artery. Hear Res 209: 91–96.
8. Vass Z, Dai CF, Steyger PS, Jancsó G, Trune DR, et al. (2004) Co-localization of the vanilloid capsaicin receptor and substance P in sensory nerve fibers innervating cochlear and vertebro-basilar arteries. Neuroscience 124: 919–927.
9. Gruber DD, Dang H, Shimozono M, Scofield MA, Wangemann P (1998) Alpha1A-adrenergic receptors mediate vasoconstriction of the isolated spiral modiolar artery in vitro. Hear Res 119: 113–124.
10. Scherer EQ, Lidington D, Oestreicher E, Arnold W, Pohl U, et al. (2006) Sphingosine-1-phosphate modulates spiral modiolar artery tone: A potential role in vascular-based inner ear pathologies? Cardiovasc Res 70: 79–87.
11. Sadanaga M, Liu J, Wangemann P (1997) Endothelin-A receptors mediate vasoconstriction of capillaries in the spiral ligament. Hear Res 112: 106–114.
12. Scherer EQ, Yang J, Canis M, Reimann K, Ivanov K, et al. (2002) Tumor necrosis factor-α enhances microvascular tone and reduces blood flow in the cochlea via enhanced sphingosine-1-phosphate signaling. Stroke 41: 2618–2624.
13. Herzog M, Scherer EQ, Albrecht B, Rorabaugh B, Scofield MA, et al. (2002) CGRP receptors in the gerbil spiral modiolar artery mediate a sustained vasodilation via a transient cAMP-mediated Ca2+-decrease. J Membr Biol 189: 225–236.
14. Jiang ZG, Shi X, Zhao H, Si JQ, Nuttall AL (2004) Basal nitric oxide production contributes to membrane potential and vasotone regulation of guinea pig in vitro spiral modiolar artery. Hear Res 189: 92–100.
15. Li L, Rose P, Moore PK (2011) Hydrogen sulfide and cell signaling. Annu Rev Pharmacol Toxicol 51: 169–187.
16. Liu X, Pan L, Zhuo Y, Gong Q, Rose P, et al. (2010) Hypoxia-inducible factor-1alpha is involved in the pro-angiogenic effect of hydrogen sulfide under hypoxic stress. Biol Pharm Bull 33: 1550–1554.
17. Yang G, Wu L, Jiang B, Yang W, Qi J, et al. (2008) H2S as a physiologic vasorelaxant: hypertension in mice with deletion of cystathionine gamma-lyase. Science 322: 587–590.
18. Mok YY, Atan MS, Yoke Ping C, Zhong Jing W, Bhatia M, et al. (2004) Role of hydrogen sulphide in haemorrhagic shock in the rat: protective effect of inhibitors of hydrogen sulphide biosynthesis. Br J Pharmacol 143: 881–889.
19. Wang R (2009) Hydrogen sulfide: a new EDRF. Kidney Int 76: 700–704.
20. Gadalla MM, Snyder SH (2010) Hydrogen sulfide as a gasotransmitter. J Neurochem 113: 14–26.
21. Olson KR (2005) Vascular actions of hydrogen sulfide in nonmammalian vertebrates. Antioxid Redox Signal 7: 804–812.
22. Webb GD, Lim LH, Oh VM, Yeo SB, Cheong YP, et al. (2007) Contractile and vasorelaxant effects of hydrogen sulfide and its biosynthesis in the human internal mammary artery. J Pharmacol Exp Ther 324: 876–882.
23. Elsey DJ, Fowkes RC, Baxter GF (2010) Regulation of cardiovascular cell function by hydrogen sulfide (H(2)S). Cell Biochem Funct 28: 95–106.
24. Wang MJ, Cai WJ, Zhu YC (2010) Mechanisms of angiogenesis: role of hydrogen sulphide. Clin Exp Pharmacol Physiol 37: 764–771.
25. Qiao W, Chaoshu T, Hongfang J, Junbao D (2010) Endogenous hydrogen sulfide is involved in the pathogenesis of atherosclerosis. Biochem Biophys Res Commun 396: 182–186.
26. Nicholson CK, Calvert JW (2010) Hydrogen sulfide and ischemia-reperfusion injury. Pharmacol Res 62: 289–297.
27. Zhang J, Sio SW, Moochhala S, Bhatia M (2010) Role of hydrogen sulfide in severe burn injury-induced inflammation in mice. Mol Med 16: 417–424.
28. Whiteman M, Haigh R, Tarr JM, Gooding KM, Shore AC, et al. (2010) Detection of hydrogen sulfide in plasma and knee-joint synovial fluid from rheumatoid arthritis patients: relation to clinical and laboratory measures of inflammation. Ann N Y Acad Sci 1203: 146–150.
29. Zuidema MY, Yang Y, Wang M, Kalogeris T, Liu Y, et al. (2010) Antecedent hydrogen sulfide elicits an anti-inflammatory phenotype in postischemic murine small intestine: role of BK channels. Am J Physiol Heart Circ Physiol 299: H1554–1567.
30. Uren JR, Ragin R, Chaykovsky M (1978) Modulation of cysteine metabolism in mice–effects of propargylglycine and L-cyst(e)ine-degrading enzymes. Biochem Pharmacol 27: 2807–2814.
31. Zhao W, Ndisang JF, Wang R (2003) Modulation of endogenous production of H2S in rat tissues. Can J Physiol Pharmacol 81: 848–853.
32. Prieskorn DM, Miller JM (2000) Technical report: chronic and acute intracochlear infusion in rodents. Hear Res 140: 212–215.